

Development of Two UWB Multiband MIMO Antennas with Enhanced Isolation and Cross-Correlation

Shrenik Sarade

Electronics Engineering Department, Walchand College of Engineering, India
shreniks2k7@rediffmail.com
(corresponding author)

Sachin Ruikar

Electronics Engineering Department, Walchand College of Engineering, India
sachin.ruikar@walchandsangli.ac.in

Received: 17 October 2022 | Revised: 4 November 2022 and 17 November 2022 | Accepted: 19 November 2022

ABSTRACT

An Ultra-Wide Band (UWB) MIMO antenna working at millimeter-wave is proposed in this research. It is composed of eight radiating elements with various shapes. It is designed with a rectangular structure and various carved slots. The carved slots are used to increase the antenna's bandwidth. The antenna's radiating elements are placed near one another, and thus, isolation is widespread. In order to improve the isolation of the MIMO antenna, parasitic elements and a defective ground structure are used. Antenna parameters such as Correlation Coefficient (CC), Envelope Correlation Coefficient (ECC), Diversity Gain (DG), and Total Active Reflection Coefficient (TARC) depend on the isolation. Parasitic elements with a rectangular form are positioned between the radiating patches. Rectangular-shaped ground structures with defects comprise the ground plane. An FR-4 substrate is used to fabricate the antenna. The analysis of the antenna shows that there is less than -14dB return loss, less than -40dB isolation, less than 0.0010 cross-correlation, less than 0.10 TARC, and higher than 500MHz bandwidth. The antenna uses a fractional bandwidth higher than 35% (UWB) for the 6GHz frequency and operates on a variety of bands. This antenna is suitable for many different wireless system applications.

Keywords-MIMO; UWB; DGS; TARC; CC; ECC; DG

I. INTRODUCTION

Modern antenna technology relies heavily on Multiple Input-Multiple Output (MIMO) antennas with several antennas in both transmitter and receiver. MIMO antenna systems increase the poor data rate of the Single Input-Single Output (SISO) system. Depending on the number of patches in the antenna, the data rate of the MIMO antenna increases linearly. Return loss, isolation, Correlation Coefficient (CC), and Total Active Reflection Coefficient (TARC) represent a MIMO antenna's performance. Multiple radiating patches are arranged on the same substrate in a MIMO antenna [1]. The radiating elements are positioned near one another. The isolation and the CC are influenced by the close proximity of the rectangular radiating patches. The data rate is reduced by the isolation. The isolation, CC, and data rate of the antennas all need to be improved. Various techniques, such as Defective Ground Structure (DGS), Parasitic Elements (PEs), metamaterials, Decoupling Structures (DSs), and Electromagnetic Band Gap (EBG) are used to increase isolation and CC. In the ground plane, carved holes of different shapes are employed in DGS

methods [2-7]. In order to promote isolation, a decoupling structure is built that isolates the input of the radiating patches from the corresponding network arrangement in [8-12]. To increase the isolation between the patches, parasitic components are utilized in [13-18]. Using the literature mentioned above, it is necessary to create a MIMO antenna that operates on a multiband application with an ultra-wide bandwidth, improved TARC, and better cross correlation. In previous works, the same shaped radiating elements were used to design an MIMO antenna, whereas the cross correlation (CC and ECC) between the radiating elements was high.

In this study, a 2-MIMO antenna with a variety of shapes is proposed. The antenna is developed using radiating elements of different shapes. The designed antenna operates on a multiband and its bandwidth is UWB. For bandwidth improvement, a rectangular shaped cut slot is introduced between the radiating elements of the antenna. The isolation between the radiating elements is improved using DGS and PEs. Antenna parameters such as isolation, cross correlation (CC and ECC), and TARC depend on isolation.

The novelty of the current work is that the radiating elements are developed in different shapes, the rectangular shaped DGS cut slot and PEs are designed for the improvement of isolation, CC, ECC, TARC, and DG. For the improvement of the bandwidth, different rectangular cut slots are designed and introduced in the radiating elements.

II. DESIGN OF A MASSIVE MIMO ANTENNA USING DEFECTIVE GROUND STRUCTURE (DGS)

In this section, the design of the massive MIMO antenna is explained in detail. The designed antenna comprises 8 rectangular radiating patches with distinct cut slots for the 6GHz frequency with the antenna dimensions, as shown in Figure 1. The antenna is analyzed and fabricated using an FR-4 substrate with 1.6mm height (h) and 4.4 dielectric constant. The radiating element's geometrical features, such as length

(L_p) and width (W_p) have been created using the rectangular radiating patch transmission line model [21-23] (Table I). Table I shows the measurements of the 8 radiating elements with varying cut slots. A rectangular cut slot [21-22] is placed in the radiating elements P_1 to P_8 . Patch 1 has rectangular cut slots-1 and 2 (CS-1 and 2). Patches 2, 3, and 7 have the rectangular cut slot-2. Cut slot-3 is placed in patches 6 and 8. In patch 4, rectangular cut slot-1 is introduced. Patch 5 introduces rectangular cut slots-1 and 3 (CS-1 and 3). The radiating elements of the antenna are excited using an Inset Feed Line (IFL) [21-22]. The fabricated antenna structure is shown in Figure 3. The antenna is fabricated on the FR-4 substrate. The radiating elements of the antenna are placed close to each other. Therefore, the isolation between the radiating elements is high. Isolation of the antenna affects the performance parameters of the antenna [21-22].

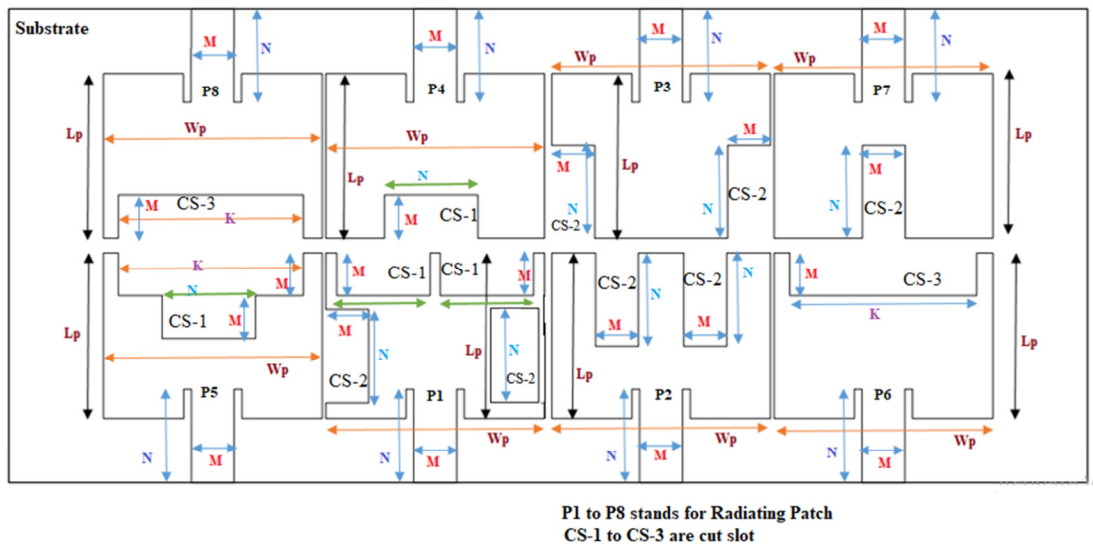


Fig. 1. The dimensions of a developed massive MIMO antenna (top side).

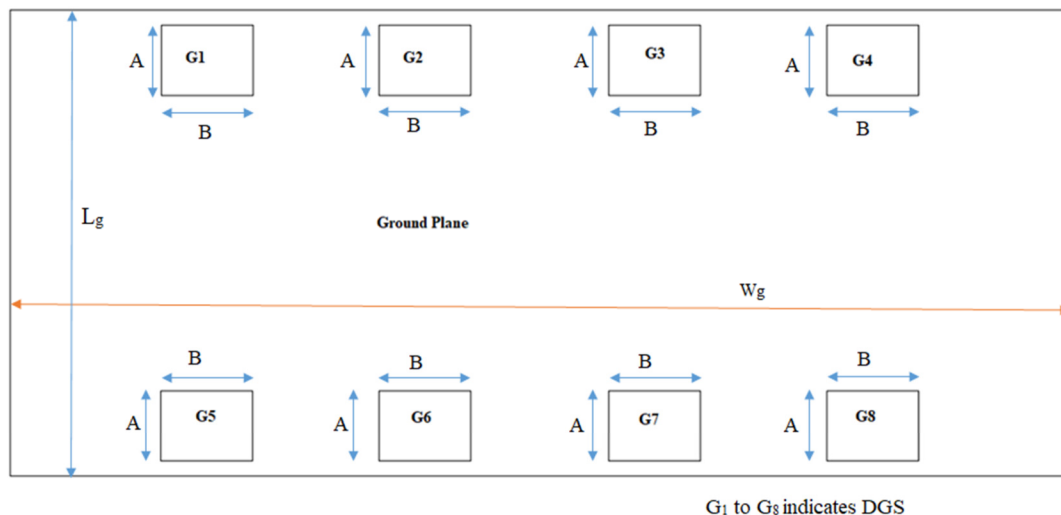


Fig. 2. The dimensions of a ground plane (back side) of the antenna.

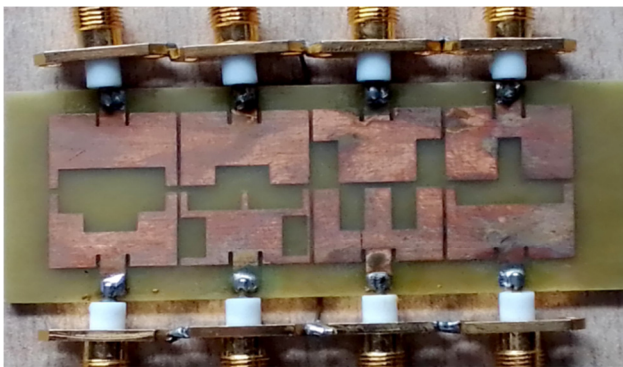


Fig. 3. Fabricated top side of a massive MIMO antenna.

TABLE I. MIMO ANTENNA DIMENSIONS

Parameter	Dimensions (mm)
Patch length (L_p)	11.38
Patch width (W_p)	15.21
Width of IFL	$N = 6.41$
Length of IFL	$M = 2.942$
Width of cut slot-1	$N = 6.41$
Length of cut slot-1	$M = 2.942$
Width of cut slot-2	$M = 2.942$
Length of cut slot-2	$N = 6.41$
Width of cut slot-3	$K = 12.69$
Length of cut slot-3	$M = 2.942$
Length of a substrate	$L_G = 32.58$
Width of a substrate	$W_G = 74$
Length of a DGS cut slot	$A = 5.884$
Width of a DGS cut slot	$B = 6.38$

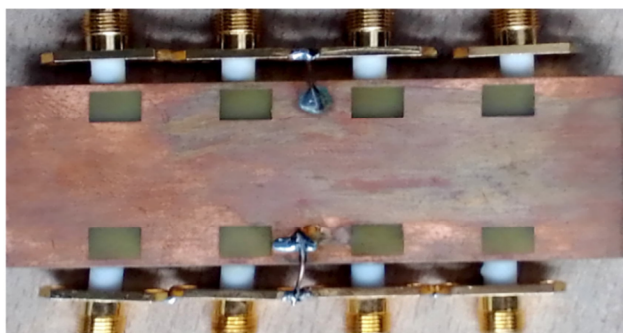


Fig. 4. Fabricated back side (ground plane) of a massive MIMO antenna.

Hence, there is a requirement to improve the isolation between the radiating elements. For isolation improvement, the DGS cut slots G_1 to G_8 [2-7] are introduced in the ground plane as shown in Figure 2, whereas the fabrication of the ground plane is shown in Figure 4. The dimensions of the ground plane with DGS are shown in Table I. The result analysis of the antenna (for radiating elements-1 and 4) is shown in Figures 5 and 6. The antenna parameters are tested in the Vector Network Analyser (VNA). The analysis shows -14.40dB return loss and -42.72dB isolation have been measured in the -6dB line of return loss. At the -6dB line of return loss, the antenna operates on the frequency band of 0.33GHz-7.5GHz. This antenna is operated on UWB. The Voltage Standing Wave Ratio (VSWR) is illustrated in Figure 7. The VSWR for the antenna is less than 3.65dB.

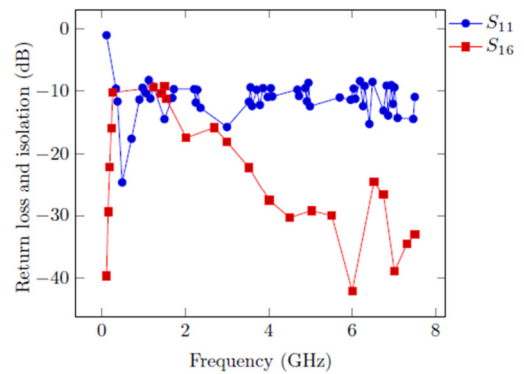


Fig. 5. Result of return loss S_{11} and isolation.

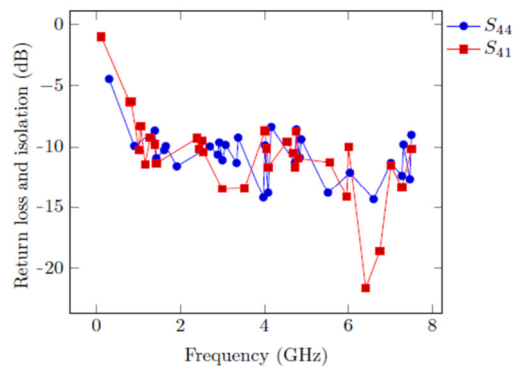


Fig. 6. Result of return loss S_{44} and isolation.

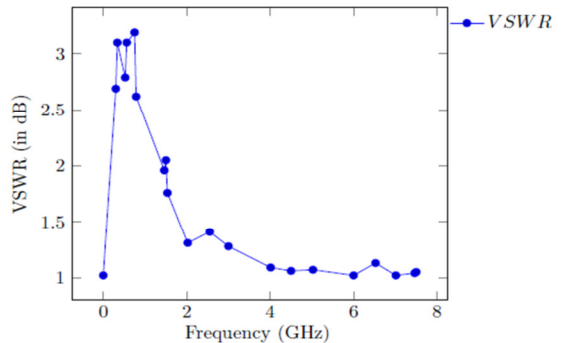


Fig. 7. VSWR of radiating elements of the antenna.

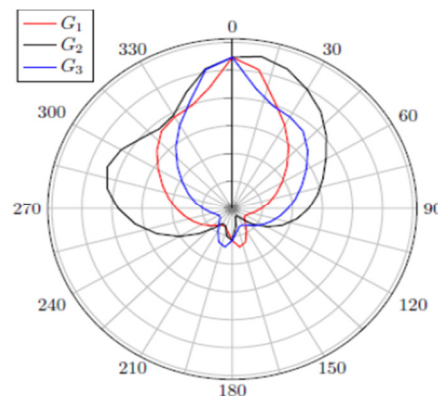


Fig. 8. Radiation pattern of the antenna.

Figure 8 shows the radiation pattern for the gain of the antenna. The gains G_1 , G_2 and G_3 of the antenna are measured at $\phi=0^\circ$, $\phi=90^\circ$ and $\phi=180^\circ$, respectively. The obtained gain of the antenna is 1.54dB. The antenna parameters, such as TARC, CC, ECC, and DG depend on the return loss and isolation [21-22]. The analysis of the antenna shows CC less than 0.153, ECC less than 0.0237, TARC less than 0.137 (-8.63dB), and 9.99 DG.

III. DESIGN OF THE MASSIVE MIMO ANTENNA USING PARASITIC ELEMENTS

In this section, the massive MIMO antenna is designed using PEs for the frequency of 6GHz as shown in Figure 10. It consists of 8 radiating elements (Patch 1 to 8), which are designed using a rectangular shaped transmission line model [21-23]. Radiating elements 2, 4, 7, and 8 have rectangular cut slots. The radiating elements are placed close to each other and the isolation between them is high. For the isolation enhancement between the radiating elements, rectangular shaped PEs (P_1 to P_{14}) are placed among them [21-23]. The dimensions of the antenna are shown in Figure 9 and Table II. The PEs are used to negate parts of the coupled field between the radiating elements because they create the opposite coupling field, which lessens the original field and hence reduces the total coupling on the antenna. The PE structure and the radiating patch are not physically related [22]. Figure 9 exhibits the fabricated antenna (top side). This antenna is fabricated on the FR-4 substrate which has a 4.4 dielectric constant and 1.6mm height. The fabricated ground plane (back side) of the antenna is shown in Figure 11. The ground plane has 36.522mm length (L_{SUB}) and 90mm width (W_{SUB}). The result analysis of the antenna (for radiating elements-2 and 6) is shown in Figures 12 and 13. The antenna parameters are tested in the VNA. The measured return loss and isolation in the -6dB line of return loss are -13.96dB and -46.46dB, respectively. At the

-6dB line of return loss, the antenna operates on two frequency bands, namely, 0.82-1.76GHz and 3.03-7.5GHz. This antenna operates on UWB. Figure 14 shows the radiation pattern of the gains of the antenna. The gains G_1 , G_2 and G_3 of the antenna are measured at $\phi=0^\circ$, $\phi=90^\circ$, and $\phi=180^\circ$, respectively. The obtained gain of the antenna is 2.73dB. The ECC is less than 0.001, CC is less than 0.01, DG is close to 10, and TARC is less than 0.015 (-8.23dB) [21-23].

TABLE II. DIMENSIONS OF A MASSIVE MIMO ANTENNA USING PES

Parameter	Dimensions (mm)
Patch length (L_{rp})	11.34
Patch width (W_{rp})	15.234
Width of IFL	$B = 6.41$
Length of IFL	$A = 2.942$
Width of cut slot	$B = 6.41$
Length of cut slot	$A = 2.942$
PE width (P_1 to P_{10})	$D = 2.942$
PE length (P_1 to P_{10})	$C = 11.34$
PE width (P_{11} to P_{14})	$E = 15.234$
PE length (P_{11} to P_{14})	$D = 2.942$
Length of substrate	$L_{SUB} = 36.522$
Width of substrate	$W_{SUB} = 90$

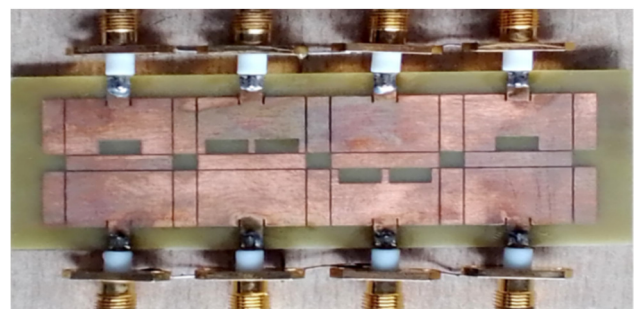
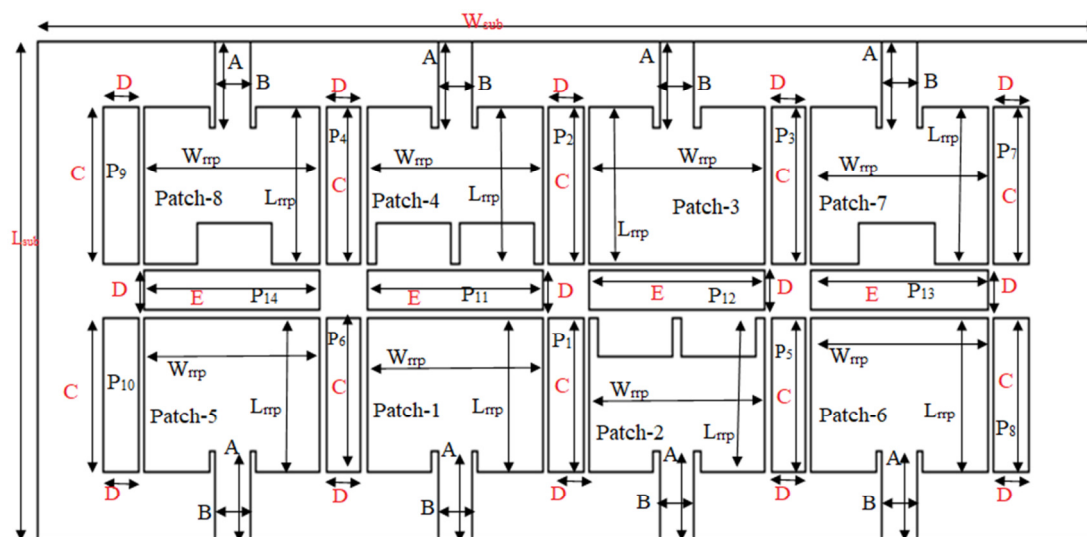


Fig. 9. The fabricated MIMO antenna (top side).



P_1 to P_{14} are indicates that parasitic elements

Fig. 10. Dimensions of the massive MIMO antenna using PEs.

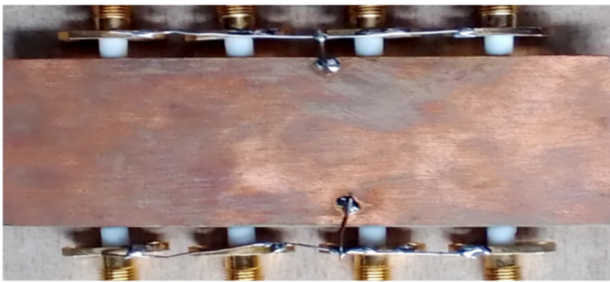


Fig. 11. The fabricated MIMO antenna (back side-ground plane).

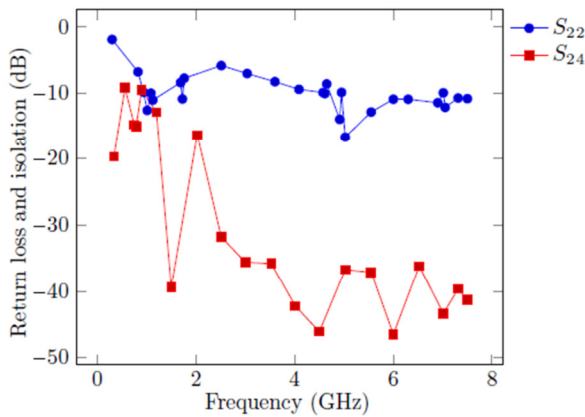


Fig. 12. Result analysis of return loss S_{22} and isolation.

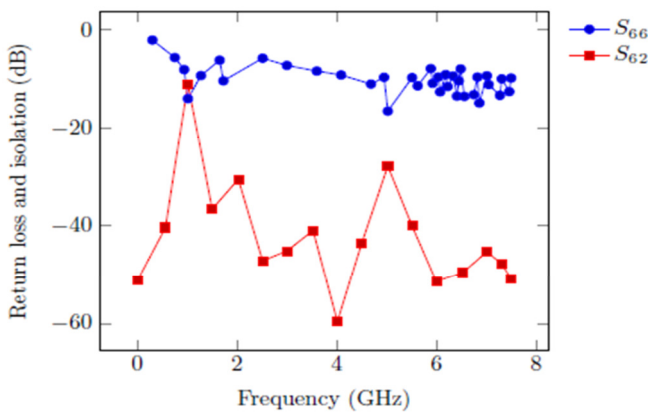


Fig. 13. Return loss S_{66} and isolation.

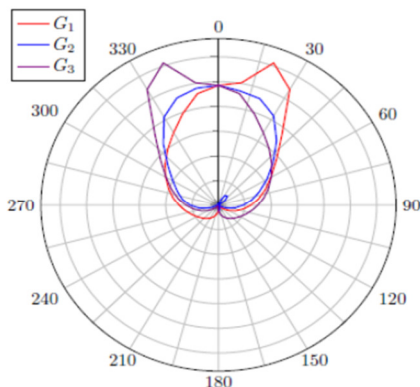


Fig. 14. Radiation pattern of the antenna.

IV. ANTENNA PERFORMANCE COMPARISON

The major contribution of the designed antenna is the different-shaped radiating elements. The antenna parameters are enhanced using two different techniques, namely, DGS and PEs. The designed antenna can operate on various UWB applications. The analysis shows that the cross correlation and TARC are better than the ones reported in previous research works. The comparison of the proposed antenna parameters with the other research works is shown in Table III. The proposed antenna is developed with 8 differently shaped radiating elements. It operates on a multiband frequency with a wide bandwidth.

TABLE III. COMPARISON OF THE PROPOSED WORK WITH OTHER WORKS

Ref	Method	Parameter values	Frequency band and bandwidth	Radiating patches
[2]	DGS	-10 dB RL, -12dB isolation	Single band and narrow band	8 same shaped radiating patches
[8]	DS	-20 dB RL, -15dB isolation	Dual band and narrow band	8 same shaped radiating patches
[13]	PE	-10 dB RL, -10dB isolation	Dual band and wide band	8 same shaped radiating patches
Proposed (section II)	DGS	-14.40 dB RL, -42.72dB isolation	0.33-7.5GHz and UWB with better cross correlation	8 radiating patches of different shapes
Proposed (section III)	PE	-13.96 dB RL, -46.46dB isolation	0.82-1.76GHz and 3.03-7.5GHz and UWB with better cross correlation	8 radiating patches of different shapes

V. CONCLUSION

In this paper, two MIMO antennas were designed. First, an antenna was developed using the DGS technique. The isolation, CC, ECC, TARC, DG, and channel capacity of the antenna were enhanced with the use of DGS. The DGS cut slots were introduced in the ground plane of the antenna. The analysis shows -14.40dB return loss and -42.72dB isolation measured in the -6dB line of return loss. At that line, the antenna operates on the frequency band of 0.33-7.5GHz. This antenna is operated on multiband applications with ultra-wide bandwidth.

Another antenna was developed using PEs. The antenna parameters CC, isolation, ECC, TARC, DG, and channel capacity were enhanced. The PEs were placed between the radiating elements. The analysis shows -13.96 dB return loss and -46.46dB isolation measured in the -6dB line of return loss, in which the antenna operates on two frequency bands, namely 0.82-1.76GHz and 3.03-7.5GHz.

REFERENCES

[1] Z. A. Shamsan, "Statistical Analysis of 5G Channel Propagation using MIMO and Massive MIMO Technologies," *Engineering, Technology & Applied Science Research*, vol. 11, no. 4, pp. 7417-7423, Aug. 2021, <https://doi.org/10.48084/etasr.4264>.
 [2] Y. Li, C.-Y.-D. Sim, Y. Luo, and G. Yang, "High-Isolation 3.5 GHz Eight-Antenna MIMO Array Using Balanced Open-Slot Antenna

- Element for 5G Smartphones," *IEEE Transactions on Antennas and Propagation*, vol. 67, no. 6, pp. 3820–3830, Jun. 2019, <https://doi.org/10.1109/TAP.2019.2902751>.
- [3] A. A. Megahed, M. Abdelazim, E. H. Abdelhay, and H. Y. M. Soliman, "Sub-6 GHz Highly Isolated Wideband MIMO Antenna Arrays," *IEEE Access*, vol. 10, pp. 19875–19889, 2022, <https://doi.org/10.1109/ACCESS.2022.3150278>.
- [4] M. M. El-Wazzan, H. H. Ghouz, S. K. El-Diasty, and M. A. Aboul-Dahab, "Compact and Integrated Microstrip Antenna Modules for mm-Wave and Microwave Bands Applications," *IEEE Access*, vol. 10, pp. 70724–70736, 2022, <https://doi.org/10.1109/ACCESS.2022.3187035>.
- [5] J. C. Dash and D. Sarkar, "Microstrip Patch Antenna System With Enhanced Inter-Port Isolation for Full-Duplex/MIMO Applications," *IEEE Access*, vol. 9, pp. 156222–156228, 2021, <https://doi.org/10.1109/ACCESS.2021.3128997>.
- [6] M. O. Dwairi, "Increasing Gain Evaluation of 2x1 and 2x2 MIMO Microstrip Antennas," *Engineering, Technology & Applied Science Research*, vol. 11, no. 5, pp. 7531–7535, Oct. 2021, <https://doi.org/10.48084/etasr.4305>.
- [7] P. Kumar *et al.*, "Design of a Six-Port Compact UWB MIMO Antenna With a Distinctive DGS for Improved Isolation," *IEEE Access*, vol. 10, pp. 112964–112974, 2022, <https://doi.org/10.1109/ACCESS.2022.3216889>.
- [8] L. Cui, J. Guo, Y. Liu, and C.-Y.-D. Sim, "An 8-Element Dual-Band MIMO Antenna with Decoupling Stub for 5G Smartphone Applications," *IEEE Antennas and Wireless Propagation Letters*, vol. 18, no. 10, pp. 2095–2099, Jul. 2019, <https://doi.org/10.1109/LAWP.2019.2937851>.
- [9] M. Li and S. Cheung, "Isolation Enhancement for MIMO Dielectric Resonator Antennas Using Dielectric Superstrate," *IEEE Transactions on Antennas and Propagation*, vol. 69, no. 7, pp. 4154–4159, Jul. 2021, <https://doi.org/10.1109/TAP.2020.3044683>.
- [10] M. Li, M. Y. Jamal, L. Jiang, and K. L. Yeung, "Isolation Enhancement for MIMO Patch Antennas Sharing a Common Thick Substrate: Using a Dielectric Block to Control Space-Wave Coupling to Cancel Surface-Wave Coupling," *IEEE Transactions on Antennas and Propagation*, vol. 69, no. 4, pp. 1853–1863, Apr. 2021, <https://doi.org/10.1109/TAP.2020.3026897>.
- [11] Y. Luo, T. Yin, N. Yan, W. An, and K. Ma, "A Low-Cost Differentially Fed Dual-Mode Filtering MIMO Antenna With Enhanced Isolation Based on SISL Platform," *IEEE Antennas and Wireless Propagation Letters*, vol. 21, no. 1, pp. 198–202, Jan. 2022, <https://doi.org/10.1109/LAWP.2021.3124970>.
- [12] T. Pei, L. Zhu, J. Wang, and W. Wu, "A Low-Profile Decoupling Structure for Mutual Coupling Suppression in MIMO Patch Antenna," *IEEE Transactions on Antennas and Propagation*, vol. 69, no. 10, pp. 6145–6153, Jul. 2021, <https://doi.org/10.1109/TAP.2021.3098565>.
- [13] N. O. Parchin *et al.*, "Eight-Element Dual-Polarized MIMO Slot Antenna System for 5G Smartphone Applications," *IEEE Access*, vol. 7, pp. 15612–15622, 2019, <https://doi.org/10.1109/ACCESS.2019.2893112>.
- [14] Y.-F. Tsao, A. Desai, and H.-T. Hsu, "Dual-Band and Dual-Polarization CPW Fed MIMO Antenna for Fifth-Generation Mobile Communications Technology at 28 and 38 GHz," *IEEE Access*, vol. 10, pp. 46853–46863, 2022, <https://doi.org/10.1109/ACCESS.2022.3171248>.
- [15] S. Yang, L. Liang, W. Wang, Z. Fang, and Y. Zheng, "Wideband Gain Enhancement of an AMC Cavity-Backed Dual-Polarized Antenna," *IEEE Transactions on Vehicular Technology*, vol. 70, no. 12, pp. 12703–12712, Sep. 2021, <https://doi.org/10.1109/TVT.2021.3119643>.
- [16] A. E. Farahat, K. F. A. Hussein, and M. Abo. El-Hassan, "Design Methodology of Multiband Printed Antennas for Future Generations of Mobile Handsets," *IEEE Access*, vol. 10, pp. 75918–75931, 2022, <https://doi.org/10.1109/ACCESS.2022.3192548>.
- [17] Z. Chen, W. Zhou, and J. Hong, "A Miniaturized MIMO Antenna With Triple Band-Notched Characteristics for UWB Applications," *IEEE Access*, vol. 9, pp. 63646–63655, 2021, <https://doi.org/10.1109/ACCESS.2021.3074511>.
- [18] Z. Han, S. Shen, Y. Zhang, C.-Y. Chiu, and R. Murch, "A Pattern Correlation Decomposition Method for Analysis of ESPAR in Single-RF MIMO Systems," *IEEE Transactions on Wireless Communications*, vol. 21, no. 7, pp. 4654–4668, Jul. 2022, <https://doi.org/10.1109/TWC.2021.3131612>.
- [19] H. Alsaif, "Extreme Wide Band MIMO Antenna System for Fifth Generation Wireless Systems," *Engineering, Technology & Applied Science Research*, vol. 10, no. 2, pp. 5492–5495, Apr. 2020, <https://doi.org/10.48084/etasr.3413>.
- [20] P. Bora, P. Pokkunuri, and B. T. P. Madhav, "The Design of Closed Square RR Loaded 2-Port MIMO for Dual Band Applications," *Engineering, Technology & Applied Science Research*, vol. 12, no. 2, pp. 8382–8387, Apr. 2022, <https://doi.org/10.48084/etasr.4760>.
- [21] S. S. Sarade and S. D. Ruikar, "A Different Shaped Radiating Element Wide Band Multi-Band Massive MIMO Antenna for 5G/WLAN applications with Enhanced Correlation Coefficient," *IOP Conference Series: Materials Science and Engineering*, vol. 1187, no. 1, Jun. 2021, Art. no. 012017, <https://doi.org/10.1088/1757-899X/1187/1/012017>.
- [22] S. Sarade and S. R. Ruikar, "Development of a Wide Bandwidth Massive Eight Dissimilar Radiating Element Multiband MIMO Antenna for mm-Wave Application," *Engineering, Technology & Applied Science Research*, vol. 12, no. 5, pp. 9166–9171, Oct. 2022, <https://doi.org/10.48084/etasr.5133>.
- [23] C. A. Balanis, *Antenna Theory: Analysis and Design*, 3rd ed. Hoboken, NJ, USA: Wiley, 2005.

AUTHORS PROFILE



Shrenik Sarade has received the degree in Electronics Engineering from PVPIT, Budhagaon, Sangli, under the aegis of Shivaji University, Kolhapur, in 2007. He has received the postgraduate degree in Electronics Engineering from TKIET, Warananagar, Shivaji University, and Kolhapur, India in 2014. He is pursuing his PhD in Electronics Engineering under WCE, Sangli, affiliated to Shivaji University, Kolhapur.



Sachin Ruikar has received the degree in Electronics and Telecommunication from GCE, Aurangabad, in 1998. He has received a postgraduate degree in Electronics and Telecommunication Engineering from COEP, Pune University, India in 2002. He has completed his PhD in Electronics in the Shri Guru Gobind Singh Institute of Engineering Technology, SRTMU Nanded, in 2013. Presently, he is working as an Associate Professor in Electronics Engineering at WCE, Sangli, India. His research interests include image denoising with wavelet transforms, image fusion, image painting, and image superresolution.